energies

MDPI

Article

Wireless Energy Harvesting with Cooperative Relaying under the Best Relay Selection Scheme

Admoon Andrawes, Rosdiadee Nordin * and Mahamod Ismail

Centre of Advanced Electronic and Communication Engineering, Faculty of Engineering and Built Environment, Universiti Kebangsaan Malaysia, 43600 Bangi, Selangor, Malaysia; andrawes2013@gmail.com (A.A.); mahamod@ukm.edu.my (M.I.)

* Correspondence: adee@ukm.edu.my; Tel.: +60-3-8911-8402

Received: 23 November 2018; Accepted: 2 January 2019; Published: 7 March 2019

Abstract: One of the most notable challenges in wireless communications is energy scarcity, which has attracted considerable attention in Fifth Generation (5G) wireless network research. This paper investigates the performance of energy harvesting (EH) relays under the best relay selection (BRS) scheme. The results show degradation of spectral efficiency (SE) due to EH relaying compared with conventional cooperative relaying (CR). Conversely, EH relaying provides a positive gain compared with conventional CR, increasing the lifetime of the network and decreasing energy consumption (EC) and operational cost. Moreover, the EH relaying network has better energy efficiency (EE) compared with conventional relaying networks. Results show that when EH relaying is applied, EE is improved through an increased number of relays. Finally, the SE-EE metric is presented for both conventional and EH relays. Results show that the performance of the proposed technique was able to achieve a maximum SE of 1.4 bits/s/Hz and maximum EE at 0.6 bits/s/Hz, and for the case of conventional relays, a maximum SE of 2 bits/s/Hz and EE at 1.1 bits/s/Hz. This result implies that the proposed EH scheme provides an optimum solution for energy-constrained wireless CR systems.

Keywords: energy harvesting; simultaneous wireless information and power transfer; outage probability; spectral efficiency; energy efficiency

1. Introduction

Cooperative relaying (CR) provides a significant enhancement of energy-efficient transmission techniques by mitigating fading [1]. The CR system sends the signal via orthogonal channels to prevent interference among the source and relay links. Significant focus has been given to multi-hop relaying in industry and academia due to many benefits such as system capacity, improved coverage, battery life, and throughput [2]. The most well-known relaying strategies are amplify-and-forward (AF) and decode-and-forward (DF) [3]. DF decodes, re-modulates, and retransmits the received signal, while AF retransmits and amplifies signals without having to decode. The DF complexity compared to AF relays significantly high due to its full processing capability. The DF protocol also needs a sophisticated media access control layer, while this is not necessary for the AF protocol [4]. On the other hand, a hybrid relaying protocol can be used in certain applications [5,6]. However, there are several limitations of the AF relays, such as non-linear distortion and noise added by the information receiver.

In numerous extreme situations, replacing or recharging the traditional power supply is impossible [7]. For instance, mobile devices implanted in patients to record health data are increasing in number; however, these devices are expensive, and their batteries can be difficult to replace. This issue has increased the demand for wireless battery charging using external sources, which then fuelled the emergence of EH. Some studies have suggested that thermoelectric, wind, and solar power could be utilized as external power sources to charge batteries wirelessly [8]. The conventional energy

harvesting (EH) technologies depend on external energy sources like wind, vibration and solar which are not always available and suffers from the time-varying issue and material inefficiency. EH using radio-frequency (RF) is an alternative approach, since RF signals carry energy as well as information without continuous monitoring and maintenance.

Wireless networks have developed considerably in terms of energy efficiency (EE). This development is driven by the needs of subscribers, design issues, satisfaction, and recently, the impact on the environment. Various measures have been employed to achieve high signal to noise ratio (SNR) without increasing the transmission power. Advanced measures include power reduction with sleep and active modes [9], having various transfer nodes that are based on payload size, interference reduction that results from poor frequency planning, device selection based on transmission distance, and many other energy-efficient transmission techniques [10]. The above measures have been used in various wireless fields based on environmental conditions and payload applications. One of the advanced techniques relies on exploiting the RF signals that are radiated from the ambient transmitter, known as the simultaneous wireless information and power transfer (SWIPT) network. SWIPT allows effective resource allocation at transceiver designs, which collectively form the potential 5G network technology [11]. Limited battery life in the conventional CR results in a short network lifetime. Traditional EH sources, such as thermal, solar, and wind, are not always available because of their seasonality, low efficiency, and dependency on surrounding nature, which contributes to the decrease of wireless network reliability due to network outages [12]. The use of RF signals for SWIPT has recently become a valuable EH source due to its capability to carry information and energy simultaneously.

One of the major performance indicators of the Third Generation Partnership Project (3GPP) evolution is the maximum value of spectral efficiency (SE). A typical example is an increment in the target downlink SE of 3GPP from 0.05 to 5 bits/s/Hz due to the evolution of the mobile system from Global System for Mobile (GSM) to Long Term Evolution (LTE). In contrast, EE has not been recognized by researchers and was not taken into consideration by 3GPP to indicate its performance until recent times. The continuous promotion of green energy has drawn more attention to energy-efficient transmission. Hence, the trade-off between SE and EE demands a critical study to achieve a balance between the two performance metrics in future wireless systems [13]. Based on the literature review, choosing the EH relay that minimizes the total energy consumption (EC) and then illustrating the SE-EE metric for EH relay in this scenario has not been investigated yet. Therefore, we study SE and EE design in N-EH relay networks. A direct link and the outage probability (OP) are taken into consideration. In this work, an efficient algorithm is derived to achieve individual constraints and minimize the total EC, depending on the objective function. The EE is formulated as an optimization problem with a specific objective function to minimize the total EC under maximum energy constraint and a threshold constraint for SNR. The novelty and technical contribution in this study can be summarized as follows:

(i) Analysis of the outage probability (OP) for AF-EH relaying under best relay selection (BRS) scheme with SWIPT technique, by computing the OP for the direct path and the OP for the best relay path. The EH relay can be more valuable over small areas. Consequently, the proposed system is considered in which the source, relays and destination are located in a small territory. In this case, outage probability will be beneficial due to the restrictions decreed on the relays by the energy constraints.
(ii) Investigation of the performance of total consumed energy for AF wireless energy harvesting (WEH) relaying under BRS scheme, by minimizing the total EC to improve EE for EH relaying over conventional relaying.
(iii) Derivation of the energy efficiency (EE) for AF-EH relaying, taking into account the outage probability factor and compare the results with conventional cooperative relaying with a different number of relays. Also, the effect of the power-splitting ratio on the EE is applied and the steady-state convergence is shown for different values of the power-splitting ratio.

(iv) The SE-EE trade-off is analysed for both conventional and EH relays, with the aim of optimizing the total energy consumption, by illustrating the design of the wireless networks that consider only SE and the design of the wireless networks that consider only EE. The SE-EE metric is useful in the design of required wireless EH networks to quantify the desired SE and EE.

The rest of this paper is organized as follows. Section 2 discusses recent previous studies. Section 3 describes the system model in this study. In Section 4, performance analysis for energy harvesting (EH) relaying is presented. Numerical results are presented in Section 5 and conclusions are made in Section 6.

Following notations is used in this manuscript: γ_m is the SNR thresholds for link adaptation, γ_{si} is instantaneous SNR between S and R_i, γ_{id} is the instantaneous SNR between R_i and D, γ_{sd} is the SNR of the direct path between S and D, γ_{brs} is the SNR of the best relay selection, γ_T is the combined SNR at the D, Γ^{th} is the SNR threshold.

2. Related Works

The authors of [14] presented two schemes for wireless information and power transfer: Power Splitting (PS) and Time Switching (TS). In the PS scheme, the receiver divides the signal power into two parts for harvesting energy and decoding information, while the receiver switches between two parts in the TS scheme. The authors of [15] proposed a joint analysis of the EE and SE trade-off, involving issues such as the multi-objective optimization problem (MOP). The parameters for the trade-off in the MOP change dramatically among various scenarios of communication considering different design requirements. MOP was transformed into a single-objective optimization problem (SOP) using a weighted sum algorithm, and the authors thus were able to achieve an optimal solution. In solving SOP, the harness was found as a result of the combination of channel allocation indicators.

A multi-hop wireless network consisting of the DF relay was considered in [16]. Three SWIPT general protocols were considered in this paper: TS, PS, and hybrid protocol. In each protocol, an optimization problem was formulated to decide the optimal TS and PS ratios to maximize end-to-end throughput. A best cooperative mechanism for EE and wireless spectrum sharing within 5G systems was proposed in [17]. Data were transferred, and EE was derived during the transmission mode of the intended timeslot. EH within the best cooperative mechanism was simultaneously conducted by primary users (PUs) and secondary users (SUs) from ambient signals. A short time duration with the BCM was allowed to transfer data throughout the time slot. Optimization problems were then formulated with the best cooperative mechanism model. The purpose of the optimization was to maximize the throughput for PUs and SUs under the EE metric and data rate.

In [2], an approximate mathematical expression for symbol error probability within cooperative communication systems by means of best relay selection was derived over channels of Nakagami-m fading type with independent and non-identically distributed (i.ni.d) links. In the case of AF relaying protocol, the best instantaneous SNR corresponding to the relaying link is provided by the selected relay. Differently, in the case of DF, the selected relay offers the most excellent instantaneous SNR corresponding to the link that connects the destination and the relay from the relays that have decoded the source information correctly. Joint power allocation and relay selection schemes for throughput maximization were proposed in [18] for the AF cooperative network, in which the relay and source are EH nodes. The optimal selection of the relay depends on the amount of harvested energy stored within the SNR of the nodes and channel. Offline schemes are important in case the amount of energy harvested and the SNR of the channel are given a priori, which is impossible due to the random nature of these values.

As an application of EH, the authors of [19] proposed a multi-dimensional sparse-coded ambient backscatter communication system for the high-rate massive Internet of Things (IoT) networks. RF tags were considered to increase the dimension of the signal space of backscatter signals to achieve high diversity gains. The authors guaranteed sufficient energy harvesting opportunities at RF tags. Another alternative power source from the wireless transmission can be exploited by the

use of near-field wireless power transfer (WPT), as presented in [20]. WPT has been used in mobile phones, electric vehicles, medical implants and wireless sensor network. The authors provided recent studies for near-field WPT for potential applications in the real world. Within wireless-powered communication networks (WPCNs), it is essential to search for the fairness of EE to investigate the node balance for harvesting energy and receiving information. In [21], an efficient iterative method was proposed for the fairness of optimal EE within WPCNs. The major idea was to employ stochastic geometry in deriving the mean proportional fairness utility function (PFUF) with respect to the receiver threshold and the associated probability of the user. The relaxed PFUF exhibited a concave function for the receiver threshold and the associated probability of the user. The alternative optimization approach was also used in the proposed suboptimal algorithm. The numerical results confirmed the effectiveness of the suboptimal algorithm with less computational complexity than recent related schemes. In [22], indoor EH relaying was applied over Log-Normal fading channels, a single relay was assumed. The performance of wireless transfer of the power for two-hop cooperative networks was investigated within indoor channels that have the log-normal fading distribution. Particularly, the authors considered two EH protocols, which are the PS scheme and TS scheme. They obtained precise analytical expressions for the ergodic outage probability and ergodic capacity for the previously mentioned protocols. The results illustrated that superior ergodic capacity is obtained when the channel variance is increased. The authors of [23] stated that CR is a promising technique that enhances the EE of cellular networks. However, the saved energy via deployed relays may be canceled by the static power consumption of the relay. EH is one of the techniques used for relays within cellular networks for flexible deployment and energy charge reduction.

Cognitive radio was proposed to encourage the utilization of the spectrum via exploiting the existence holes of spectrum opportunistically. The authors of [24] considered the CR among secondary users to enhance the diversity of the spectrum. A spectrum-rich user node is chosen as the relay node to enhance the performance among the destination and the source. Cooperative communication was proposed to achieve better performance for the wireless network compared to traditional wireless networks. A great deal of attention and importance has been given to these networks since they can be used in different types of networks and applications, such as: military, cellular and ad-hoc/sensor networks. In [25], the OP behavior was investigated for a cooperative network over a wireless channel with a Nakagami-m fading type. The authors derived a closed-form expression for the OP. The authors of [26] analyzed threshold-based selection combining (SC) and threshold-based maximal ratio combining (MRC) the signals of these multiple antenna Nakagami fading channels. They discovered that the end-to-end (E2E) network error performance with few number of relays and many antennas is not considerably worse compared to that who own many relays everyone has a less number of antennas. In [27], precise ergodic capacity for different adaptive protocols in DF system under different Rician fading channels was studied for optimal rate adaptation with constant power, optimal rate adaptation and simultaneous power, channel inversion based fixed rate. Through capacity analytical expressions, the optimal rate adaption and power offers superior capacity compared to optimal rate adaption by means of constant power over different Rician channels from low to reasonable SNR.

In [28], spectrum sensing for cognitive radio scenarios was proposed, and the communication frame classified based on the orthogonality and the ability of th ecooperative channel. In order to do thiy, four protocols were investigated: multiple access channel (MAC), parallel access channel (PAC), cooperative MAC (CMAC) and cooperative PAC (CPAC). Channel-aware binary-decision fusion over a shared Rayleigh flat-fading channel with multiple antennas at the Decision Fusion Center (DFC) was proposed in [29]. Two approaches were presented, Decode-and-Fuse (DaF) and Decode-then-Fuse (DtF). Authors in [30] proposed an analysis of large-array regime at the DFC. To reduce the complexity, the authors derived Sub-optimal fusion rules. The authors of [31] presented two schemes for the cooperation. In the first scheme, the cooperating relays retransmit a weighted version of the source

data in a DF fashion. The second scheme related to cooperative jamming (CJ), while the source was transmitting, cooperating relays transmit weighted noise to confound the eavesdropper.

In [32], SE was studied over a single EH relay with the adaptive transmission technique. In [33], the current contributions of the information and communication technology (ICT) system led to the release of about 5% of the carbon dioxide into the environment. Unfortunately, this percentage is increasing as the number of smart devices increase. To reduce the impact of CO_2 energy emissions, efficient techniques need to evolve to design sustainable and eco-friendly wireless communication network [34]. Following this, EE was proposed as a metric to complement SE in evaluating the absolute transmission effectiveness of 5G cellular networks [35]. The best solution is to achieve the maximum EE and SE simultaneously, although mathematically, the metrics have proven to conflict with one another, such that the maximization of EE brings about poor performance in SE [36]. Research has shown that both EE and SE have joint consideration in achieving an efficient 5G wireless communication system in the future [37]. According to [38], EE converges to a constant, $[1/N_o ln2]$, when SE approaches zero (N_o is power spectral density of additive white Gaussian noise (AWGN)), while EE approaches zero as SE goes to infinity. The ideal relationship between SE and EE is illustrated in Figure 1. The circuit power will eliminate the monotonous relationship between SE and EE. If we take the circuit power into consideration, the SE-EE curve will become bell-shaped, as in Figure 1. Transmission features such as modulation scheme, transmission distance, and resource management are influential in the SE and EE trade-off [39]. An investigation into industrial approaches and telecommunication policies toward energy-efficient transmission will become a valuable addition; it is important for protecting the environment and promoting sustainable development for future wireless cellular systems.

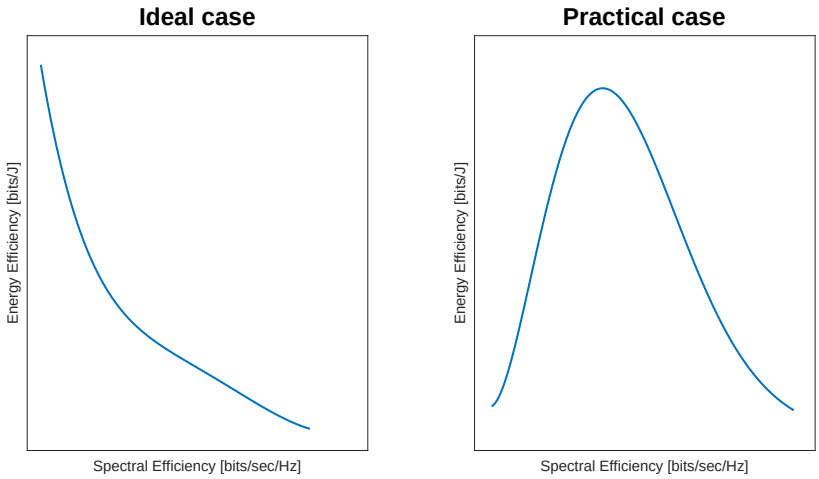

Figure 1. Ideal case and Practical case.

The authors of [40] illustrated the trade-off between performance and complexity for different combining schemes. The first scheme is defined as all relay participate (ARP), where the destination combines the received signals from all the relays, while the second scheme is known as BRS scheme, which used the relay that has the maximum signal to noise ratio (SNR) at the destination. In [41], a genetic algorithm (GA) is applied for the optimization of power splitting ratio at the relays over imperfect feedback channels. EH relaying system with link adaptation under an imperfect feedback channel was proposed in order to maximize the throughput to meet the main requirements in green wireless communication systems. The 5G innovation will soon fulfill numerous necessities, of which conveying high system energy performance is the most basic. This component is critical to decrease operational expense and give organized access in a practical and resource-efficient way. High energy performance requires a central change in outline standards inside the versatile telecom industry. The green radio networks aim to compensate for the increase in total energy consumption,

carbon footprint, and operational cost as a result from the increase in the number of base stations (BSs), which consume 57% of the total mobile network infrastructure energy [42].

Based on the previous approaches, it can be concluded that the EH relaying technique is a promising solution for achieving a green wireless system. In this paper, SE and EE of EH relaying are presented and compared with conventional relaying.

3. System Model

The CR system model is shown in Figure 2. We consider downlink EH relaying, in which a source node S sends the data to the destination node D, and the communication is applied with the help of EH relaying, R_i, $i \in \{1, 2, \ldots, N\}$ with the PS protocol. We assume a direct path between S and D with SNR, γ_{sd} with channel coefficients, h_{sd}, and distance, d_3. On the other hand, the SNR between S and R_i is denoted by $\gamma_{si} = |h_{si}|^2 E_s / N_0$ with channel coefficients, h_{si} and distance, d_1. The SNR between R_i and D is denoted by $\gamma_{id} = |h_{id}|^2 E_s / N_o$ with channel coefficients, h_{id}, and distance, d_2. All nodes are assumed to have a single antenna, and all nodes operate in a half-duplex mode. All links are assumed to undergo Rayleigh fading with perfect channel state information (CSI). In this work, the transmission process occurs in two time slots with duration T. From the AF-EH relaying, each relay is assumed to harvest a portion of the signal received by the PS protocol. A portion of the signal received by each relay is divided for information processing by a value of ρ. Thus, the rest of the signal will be represented by $1 - \rho$.

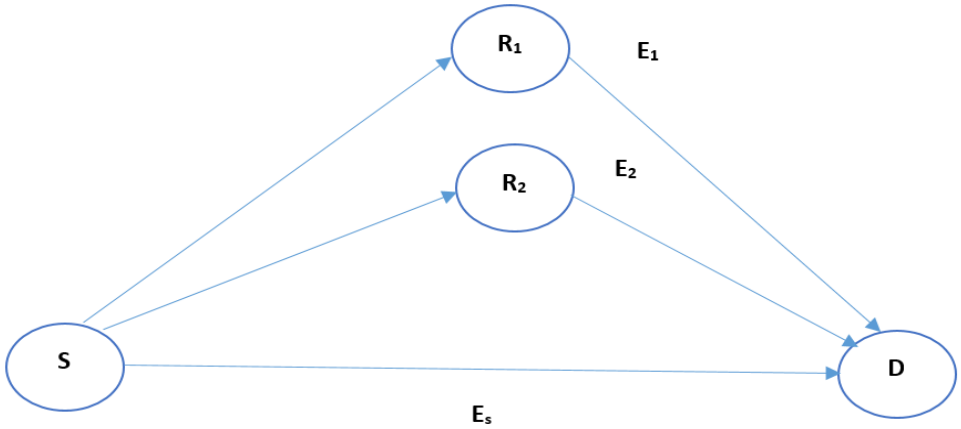

Figure 2. Downlink energy harvesting (EH) Cooperative Relaying Model with best relay selection (BRS) scheme.

3.1. Cooperative Energy Harvesting

In the case of cooperative energy harvesting, the received signal at the relay i can be written as:

$$y_{si} = h_{si} \sqrt{\frac{P_s}{{d_1}^n}} s + n_{si}, \tag{1}$$

where $n_{si} \sim CN(0, \sigma_{si}^2)$ is AWGN with noise variance, σ_{Si}^2. Assuming power splitting ratio scheme, $\sqrt{\rho} y_{si}$ is used for energy harvesting to relay i, where the remaining $\sqrt{1-\rho} y_{si}$ is used for information detection. The procedure in [43] is adopted to compute the optimized values of ρ. The harvested energy at relay i, at time $\frac{T}{2}$ can be written as

$$ER^i = \eta \rho \left[\frac{P_s}{{d_1}^n} |h_{si}|^2 \right] .T/2, \tag{2}$$

where η is the energy conversion efficiency, that depends on EH circuitry from signal power to circuit power. In this work, the energy conversion efficiency is set to 0.6, based on the assumption that the energy harvested from the received signal is not fully consumed by the relay. After power splitting, at the input of the energy harvester, the received baseband signal with information receiver noise can be written as:

$$R_{input}{}^{i} = \sqrt{1-\rho}\left[h_{si}\sqrt{\frac{P_s}{d_1{}^{n}}}s + n_{si}\right] + \dot{n}_{si}, \tag{3}$$

where $\dot{n}_{si} \sim CN(0, \dot{\sigma}_{si})$ is AWGN from the information receiver with noise variance, $\dot{\sigma}^2_{si}$. In the second time slot, the transmitted power of the relay i is given by

$$P^i_R = \frac{ER^i}{T/2} = \eta\rho\left[\frac{P_s}{d_1{}^{n}}\,|h_{si}|^2\right], \tag{4}$$

The relay amplifies and forwards the signal to the destination, the transmitted signal at the relay can be written as:

$$R_{output}{}^{i} = \frac{1}{\sqrt{d_1{}^{n}d_2{}^{n}}}\sqrt{P_s P^i_R\,(1-\rho)}Gh_{si}s + \frac{1}{\sqrt{d_2{}^{n}}}\sqrt{P^i_R}Gn_w, \tag{5}$$

where, $n_w = \sqrt{1-\rho}n_{si} + \dot{n}_{si}$, G is the gain of relay. We assumed fixed gain at all relays, G which is given as:

$$G = \frac{1}{\sqrt{\frac{(1-\rho)P_s}{d_1{}^{n}}h_{si}{}^{2} + \sigma^2_w}}, \tag{6}$$

where $\sigma^2_w = (1-\rho)\sigma^2_{si} + \dot{\sigma}^2_{si}$. The received signal at the destination can be written as

$$y_{id} = h_{id}R_{output}{}^{i} + n_{id}, \tag{7}$$

After substituting (6) and (4) into (7), the combined SNR γ_{id} can be written as below, $\sigma^2_{si} = \dot{\sigma}^2_{si} = \sigma^2_{id} = \sigma^2$ and $\bar{\gamma} = \dfrac{P_s}{\sigma^2}$.

$$\gamma_{brs} = \frac{\eta\rho(1-\rho)\bar{\gamma}^2|h_{si}|^4|h_{id}|^2 d_1{}^{-2n}d_2{}^{-n}}{\eta\rho(1-\rho)\bar{\gamma}|h_{id}|^2 d_2{}^{-n}|h_{si}|^2 d_1{}^{-n} + \eta\rho\bar{\gamma}|h_{id}|^2 d_2{}^{-n}|h_{si}|^2 d_1{}^{-n} + (1-\rho)\bar{\gamma}|h_{si}|^2 d_1{}^{-n} + (1-\rho) + 1}, \tag{8}$$

In this paper, QPSK, 16-QAM and 64-QAM are used for link adaptation according to Long Term Evolution-Advanced (LTE-A) standards [44]. Bit error rate-target ($BERT$) assumed to be 10^{-5} to be suitable for the higher modulation mode and Quality of Service (QoS) that meet the requirements for 4G network and beyond. SNR values can be divided considering $M+1$ regions, where M number of thresholds of SNR values. The thresholds can be found using [45]:

$$\gamma_m = \frac{2}{3}K_0(2^m - 1), \quad m = 2, 4, 6 \tag{9}$$

where $k_0 = -In(5\,BERT)$.

3.2. Moment Generating Function (MGF) and Probability Density Function (PDF) of BRS in EH Relaying

The combined SNR at the destination can be computed using BRS scheme, shown as:

$$\gamma_T = \gamma_{sd} + \gamma_{brs}, \tag{10}$$

MGF can be expressed as

$$M_{\gamma_T} = M_{\gamma_{sd}}(s) M_{\gamma_{brs}}(s), \tag{11}$$

For Rayleigh fading channel, $M_{sd}(s) = (1 + s\bar{\gamma}_{sd})^{-1}$, while, MGF for γ_{brs} in the case of BRS scheme for N relays can be expressed as [46]:

$$M_{\gamma_{brs}}(s) = \sum_{i=0}^{N-1} \frac{N(-1)^i \binom{N-1}{i}}{1 + i + s\gamma_{brs}/2}, \tag{12}$$

In the case of cooperative EH, MGF can be written as:

$$M_{\gamma_T}(s) = (1 + \gamma_{sd} s)^{-1} \sum_{i=0}^{N-1} \frac{N(-1)^i \binom{N-1}{i}}{1 + i + s\gamma_{brs}/2}, \tag{13}$$

using a partial fraction and taking Inverse Laplace transform with some algebraic manipulation, the PDF of γ_T can be expressed as:

$$p_{\gamma_T}(\gamma) = N \sum_{i=0}^{N-1} (-1)^i \binom{N-1}{i} \left[\frac{A_i}{\gamma_{sd}} \exp\left(-\frac{\gamma}{\gamma_{sd}} \right) + \frac{2B_i}{\gamma_{brs}} \exp\left(-\frac{2(1+i)\gamma}{\gamma_{brs}} \right) \right], \tag{14}$$

where $A_i = 1/(1 + i - \gamma_{brs}/(2\gamma_{sd}))$, $B_i = 1/(1 - (1+i)2\gamma_{sd}/\gamma_{brs})$.

3.3. Energy Status in EH Relaying

The best relay is selected to forward the data from the source to the destination by using its harvested energy. In this case, all other relay nodes will be in silent mode and the selected relay will be active. The other relays will not consume their energy, so their energy can be stored in the batteries. The selected relay that minimizes total energy consumption is selected only if at least E^{th} is stored in the batteries. The WEH relay can be active or silent at different time instants. Assume symbol duration T_s, then the EH relay consumes $P_s T_s$ to forward a frame of Λ symbols. The EH relay is called active if it has at least $PT/2$ energy which is named E^{th}, where $T = 2\Lambda T_s$.

4. Performance Analysis

4.1. Spectral Efficiency (SE)

Taking into account the presence of feedback errors, the spectral efficiency can be expressed as follows:

$$SE = \frac{1}{2} \sum_{m=1}^{M} \log_2^{(M_m)} F_m, \tag{15}$$

where F_m represents the probability of selecting the m-th modulation model for the transmission. This probability can be represented as follows: $F_m = P_\gamma(\gamma_{m+1}) - P_\gamma(\gamma_m)$, where γ_m is the threshold of SNR and $P_\gamma(\cdot)$ is the cumulative distribution function (CDF) of received SNR, which can be computed by integrating the PDF in (14).

4.2. Outage Probability (OP)

It is assumed that there are no performed transmissions below the predefined SNR threshold. The link quality is measured based on the outage probability. It is a rational measure of performance, where it is associated with the challenging slow fading channel variations [47]. The OP can be written as:

$$P_{out} = Pr\left(\max(\gamma_{sd}, \gamma_{brs}) < \Gamma^{th} \right), \tag{16}$$

Assuming i.i.d. Rayleigh fading channel, (16) can be written as:

$$P_{out} = Pr\left(\gamma_{sd} < \Gamma^{th}\right) \cdot Pr\left(\gamma_{brs} < \Gamma^{th}\right) = P_1 \times P_2, \tag{17}$$

where the first probability:

$$P_1 \quad = \quad Pr\left(\gamma_{sd} < \Gamma^{th}\right) = Pr\left(\bar{\gamma} Y < \Gamma^{th}\right) = Pr\left(Y < \frac{\Gamma^{th}}{\bar{\gamma}}\right), \tag{18}$$

where $Y = |h_{sd}|^2 d_3^{-n}$. According to the exponential distribution, the cumulative distribution function (CDF) can be written as:

$$P_1 = 1 - e^{-\frac{\Gamma^{th}}{\bar{\gamma}}}, \tag{19}$$

The second probability can be calculated as:

$$P_2 = Pr\left(\gamma_{brs} < \Gamma^{th}\right) = Pr\left(\frac{aX^2Z}{\bar{\rho}bXZ + bXZ + cX + \bar{\rho} + 1} < \Gamma^{th}\right), \tag{20}$$

where $X = |h_{si}|^2 d_1^{-n}$, $Z = |h_{id}|^2 d_2^{-n}$, $a = \eta\rho(1-\rho)\bar{\gamma}^2$, $b = \eta\rho\bar{\gamma}$, $c = (1-\rho)\bar{\gamma}$, $\bar{\rho} = 1 - \rho$. The remaining derivation of the second probability is presented in the Appendix A, and the final expression of the outage probability can be written as:

$$P_{out} \quad = \quad \left(1 - e^{-\frac{\Gamma^{th}}{\bar{\gamma}}}\right) \times \left[1 - 2e^{-g} \sum_{k=0}^{N-1} \frac{\xi^{\frac{1+k}{2}}}{k!} K_{k-1}\left(2\sqrt{\xi}\right)\right], \tag{21}$$

where $g = \frac{(2-\rho)\Gamma^{th}}{(1-\rho)\bar{\gamma}}$, $\xi = \frac{(c+\bar{\rho}+1)\Gamma^{th}}{a}$, $K_\nu(\cdot)$ is the ν-th order modified Bessel function of the second kind.

4.3. Energy Consumption (EC) for EH Relaying

The relay that has minimum EC will be selected as the best relay, so the total energy consumption will be the energy from the direct path and the energy of the i-th relay. On the other hand, a threshold SNR Γ^{th} will be defined to ensure that the rate is above a specific rate with function Γ^{th}. According to (5) with the help of (6), the total average SNR can be written as:

$$\gamma_T = \frac{E_s |h_{sd}|^2}{{d_3}^n \sigma_{sd}^2} + \frac{E_i E_s \bar{\rho} |h_{si}|^2 |h_{id}|^2 {d_1}^{-n} {d_2}^{-n}}{\frac{E_i}{{d_2}^n} \bar{\rho} |h_{id}|^2 \sigma_{si}^2 + \frac{E_i}{{d_2}^n} |h_{id}|^2 \dot{\sigma}_{si}^2 + \sigma_{id}^2 \left(\bar{\rho} |h_{si}|^2 \frac{E_s}{{d_1}^n} + \bar{\rho}\sigma_{si}^2 + \sigma_{si}^2\right)}, \tag{22}$$

Assuming $\sigma_{si}^2 = \dot{\sigma}_{si}^2, \nu_o = \frac{|h_{sd}|^2}{\sigma_{sd}^2} d_3^{-n}, \zeta_i = \frac{|h_{id}|^2}{\sigma_{id}^2} d_2^{-n}, \nu_i = \frac{|h_{si}|^2}{\sigma_{si}^2} d_1^{-n}$.

After mathematical manipulation, that can be shown in Appendix B, for BRS scheme,

$$\gamma_T = E_s\left(\nu_0 + \nu_i\right) - \frac{E_s^2 \nu_i^2 \bar{\rho} + E_s \nu_i E_i \zeta_i + E_s \nu_i \bar{\rho} + E_s \nu_i}{E_i \bar{\rho} \zeta_i + E_i \zeta_i + E_s \bar{\rho} \nu_i + \bar{\rho} + 1}, \tag{23}$$

$$\min_{E_s, E_i} E_T, \text{ s.t.} \tag{24a}$$

$$\frac{1}{2}\log_2(1 + \gamma_T) \geq \frac{1}{2}\log_2(1 + \Gamma^{th}) \tag{24b}$$

$$0 \leq E_s \leq E_s^{max} \tag{24c}$$

$$E^{th} \leq E_i \leq E_i^{max} \tag{24d}$$

where E_s^{max} and E_i^{max} are the maximum energy at the source and the maximum energy at the selected relay respectively. It can be seen from (23) that γ_T is a monotonically increasing with two variables E_s and E_i. Thus, the optimized solution of the problem is occurred when $\gamma_T = \Gamma^{th}$. According to this, E_i can be written as a function of E_s.

$$E_i = \frac{\Gamma^{th}(E_s\overline{\rho}v_i + \overline{\rho} + v_i) - v_o(E_s^2\overline{\rho}v_i + \overline{\rho}E_s + E_s)}{\zeta_i(\overline{\rho}E_s v_o + E_s\overline{\rho}v_i + E_s v_o - \Gamma^{th}\overline{\rho} - \Gamma^{th})} \tag{25}$$

where

$$\Gamma^{th}(\overline{\rho} - 1) \neq E_s(\overline{\rho}v_o + \overline{\rho}v_i + v_0).$$

we can write E_i as

$$E_i = \frac{-a_1E_s^2 + a_2E_s + a_3}{a_4E_s - a_5} \tag{26}$$

where

$$a_1 = v_0\overline{\rho}v_i \quad , \tag{27a}$$
$$a_2 = (\Gamma^{th}\overline{\rho}v_i - \overline{\rho}v_o - v_o) \quad , \tag{27b}$$
$$a_3 = \Gamma^{th}(\overline{\rho} + v_i) \quad , \tag{27c}$$
$$a_4 = \zeta_i(\overline{\rho}v_o + \overline{\rho}v_i + v_o) \quad , \tag{27d}$$
$$a_5 = \zeta_i\Gamma^{th}(\overline{\rho} - 1) \quad , \tag{27e}$$

The total consumed energy can be written as:

$$E_T = \frac{-a_1E_s^2 + a_2E_s + a_3}{a_4E_s - a_5} + E_s, \tag{28}$$

To find the optimized value of the total energy, the first derivative is applied. To check the convexity of the proposed model, the second derivative is applied as shown in the following equations.

$$\frac{\partial E_T}{\partial E_s} = \frac{-a_1a_4E_s^2 + 2a_5a_1E_s - a_5a_2 - a_3a_4}{(a_5 - a_4E_s)^2} - 1, \tag{29}$$

$$\frac{\partial^2 E_T}{\partial E_s^2} = \frac{2(a_5^2a_1 + a_5a_2a_4 + a_3a_4^2)}{(a_4E_s - a_5)^3}. \tag{30}$$

Hence, solving the equation

$$\frac{\partial E_T}{\partial E_s} = 0, \tag{31}$$

will yield two solutions for E_s and E_i

To be E_T convex, the optimal solution is the positive term for (32) and (33)

$$E_s = \frac{a_5}{a_4} \pm \frac{\sqrt{a_5^2(a_1^2 + a_1a_4) - a_5a_2(a_1a_4 + a_4^2) - a_3a_4(a_1a_4 - a_4^2)}}{a_1a_4 + a_4^2} \tag{32}$$

If we let $\Omega = \sqrt{a_5^2(a_1^2 + a_1a_4) - a_5a_2(a_1a_4 + a_4^2) - a_3a_4(a_1a_4 - a_4^2)}$, then we can find E_i from (26)

$$E_i = -\frac{a_1a_5(a_4 - 1)}{a_4^2} - \frac{a_5(a_1 + a_4)(a_1 + a_2a_4)}{a_4^2\Omega} + \frac{\pm a_1\Omega}{a_4^2(a_1 + a_4)} + \frac{a_3(a_1 + a_4)}{\pm\Omega} \tag{33}$$

4.4. Energy Efficiency for EH Relaying

The main idea behind EE scheme is to minimize the total energy consumption while preserving SNR above the threshold. EE in relaying of AF-EH is illustrated in this section. The comparison and formulation of EH relaying for end-to-end SNR are conducted with BRS scheme relaying. This task is performed with the aid of SWIPT technique. In this section, the EE of EH relaying is based on minimizing the total EC with taking the OP into account. Using the derivative from Section 4.3, the EE of the proposed system can be described as the ratio of successful data delivery to the total energy consumption, which can be written as:

$$EE = \frac{(1 - P_1)\log_2(1 + \gamma_{sd}) + (1 - P_2)\log_2(1 + \gamma_{brs})}{E_T} \tag{34}$$

The following Algorithm 1 represents the procedure of computing EE for EH relaying, taking into account the OP of the direct path and the selected relay.

Algorithm 1: EE for EH Relaying.

procedure Initialization $(E_s^{max}, E_i^{max}, \rho, \mu, \Gamma^{th})$
$Itr \leftarrow$ Number of Iterations

$$\gamma_T \leftarrow E_s(\nu_o + \nu_i) - \frac{E_s^2\nu_i^2\bar{\rho} + E_s\nu_i E_i\zeta_i + E_s\nu_i\bar{\rho} + E_s\nu_i}{E_i\bar{\rho}\zeta_i + E_i\zeta_i + E_s\bar{\rho}\nu_i + \bar{\rho} + 1}$$

For Loop:
$i \leftarrow 1 \ldots N$
IF $\gamma_T < \Gamma^{th}$
    $E_s \leftarrow E_s^{max}$
    $E_i \leftarrow E_i^{max}$
Else
    Obtain the solution $(\gamma_T = \Gamma^{th})$
    Compute the derivative of E_T with respect to E_s
    Choose the path that minimizes E_T

$$EE \leftarrow \frac{(1 - P_1)\log_2(1 + \gamma_{sd}) + (1 - P_2)\log_2(1 + \gamma_{brs})}{E_T}$$

END For Loop

5. Numerical Results

In this section, numerical results are performed to validate the proposed theoretical analysis. N-wireless energy harvesting (WEH) relays are considered based on the BRS scheme. Numerical examples are investigated. System parameters are shown in Table 1. To study the relays location on the performance, normalized distances are applied. In the following, numerical results of outage probability for different WEH relaying are shown.

Table 1. Simulation Parameters.

Parameter	Value
SNR threshold Γ^{th}	5 dB
Energy conversion efficiency η	0.6
Path loss exponent n	2
Normalized distance from S to relay i, d_1	0.3 m
Normalized distanc from S to relay i, d_2	0.7 m
Normalized distanc from S to D d_3	1 m
Maximum energy at the source E_s^{max}	3 J
Maximum energy at the selected relay E_i^{max}	3 J
Number of relays N	2, 3, 5
Bit error rate-target $BERT$	10^{-5}

In addition, the impact of using WEH relaying on the power splitting ratio, the distance between source and relays will be analyzed. The spectral efficiency and energy efficiency of EH-AF scheme is presented and compared with a different number of N-WEH relays. Finally, the comparison between conventional AF relaying and WEH-AF relaying is illustrated by understanding the trade-off between SE and EE.

It is assumed that the relays are close to the source compared to the destination with normalized distances. Since the distance from the source to relay is increasing, the energy harvested and received signal power at the relay decreases due to the path loss.

Figure 3 represents the effect of the power-splitting ratio on the SE for a single relay at 20 dB SNR. The maximum SE result is about 1.6 bits/s/Hz. Figure 3 illustrates the importance of optimizing the power-splitting ratio to achieve the best SE of the overall system using WEH relaying. When the splitting ratio is too small, only a limited amount of energy is harvested, and this can directly affect the SE performance. in contrast, when the splitting ratio is large, the energy harvested at the relay exceeds the required level, thereby decreasing the SE level.

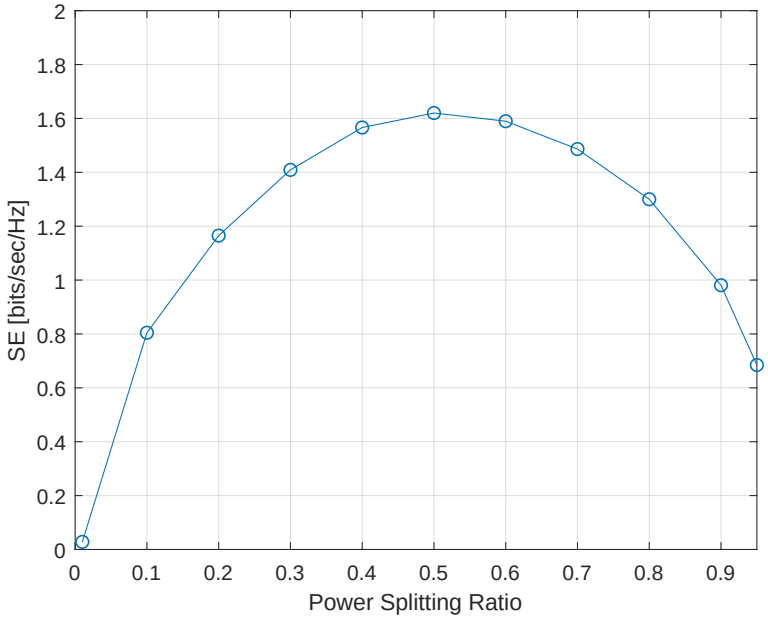

Figure 3. Spectral Efficiency (SE) at 20 dB versus the power splitting ratio.

Figure 4 shows the outage probability corresponding to average SNR with different values of N. When N increases, the outage probability is enhanced; for example, at 20 dB SNR, the outage probability for $N = 2$ is about 10^{-4}, versus about 10^{-5} at $N = 5$.

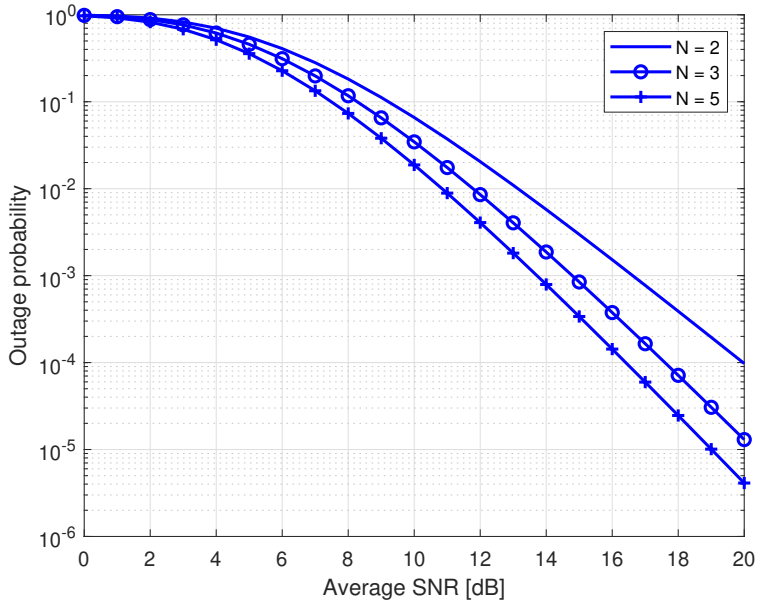

Figure 4. Outage probability versus signal to noise ratio (SNR) for EH relaying.

Figure 5 shows the outage probability results with the PS ratio for different values of N under the 5 dB SNR threshold. A portion of the power that should be received at the destination is consumed at the EH relays. Thus, the signal level that is fed to the information processing decreases with the increase in PS, which decreases the outage probability.

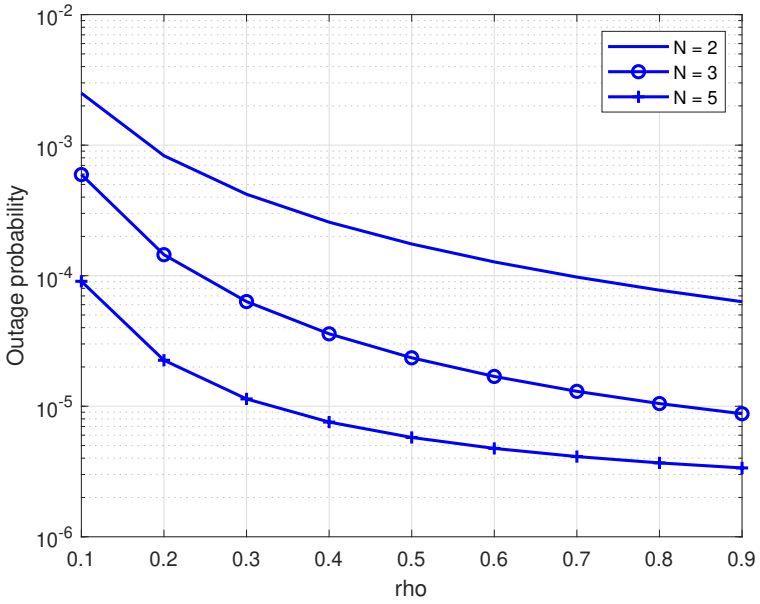

Figure 5. Outage probability versus power splitting ratio ($\bar{\gamma} = 20$ dB, $\Gamma^{th} = 5$ dB).

Figure 6 illustrates the outage probability with respect to the EH relays locations. The outage probability is constant with respect to relay locations. This occurs because at a high SNR, the outage probability becomes independent of the location of the relays.

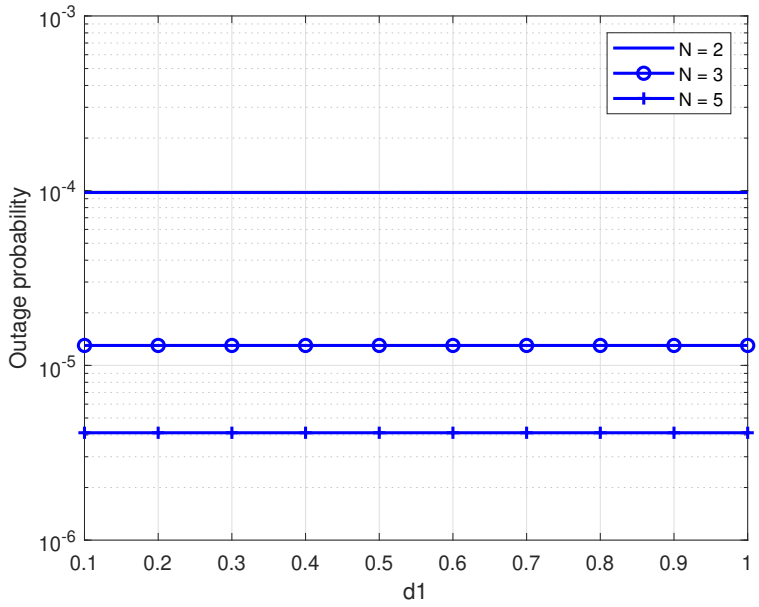

Figure 6. Outage probability versus d_1 ($\bar{\gamma} = 20$ dB, $\Gamma^{th} = 5$ dB).

Figure 7 shows the SE for conventional (non-WEH) relaying and WEH relaying. Cooperative WEH relaying causes degradation in SE compared with the conventional CR. For example, at 20 dB SNR and $N = 2$, the SE for WEH relaying is approximately 1.3 bits/s/Hz; a loss of approximately 0.4 bits/s/Hz is observed compared with the conventional CR, which translates to a 23% degradation in SE. On the other hand, increasing the number of relays enhances SE for both conventional and WEH-AF relays. For example, at 20 dB SNR with $N = 2$, SE for the conventional and WEH-AF relays are 1.7 and 1.3 bits/s/Hz, respectively, while for $N = 5$, SE for the conventional and WEH-AF relays are 2 and 1.5 bits/s/Hz, respectively. The loss occurs because of information processing from harvested energy. Previous works in this field focused on the degradation of SE due to WEH. For example, in [48], researchers proposed SWIPT for orthogonal frequency division multiplexing (OFDM), and degradation in SE reached approximately 40%.

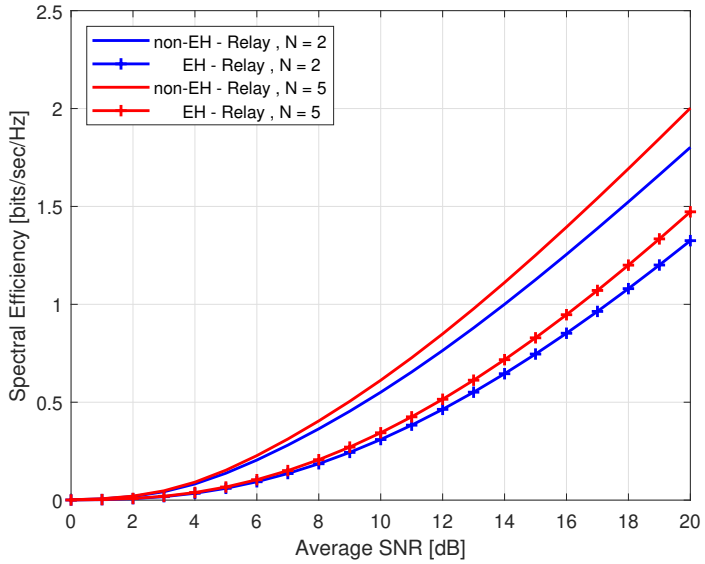

Figure 7. SE of conventional and wireless energy harvesting (WEH) relaying for the best relay selection (BRS) scheme.

Figure 8 represents the effect of the power-splitting ratio on the EE for PS protocol, The EE decreases as ρ increases from 0.1 to 0.9, for example, when $\rho = 0.1$ means that 0.9 of the transmitted power from the relay will reach to the destination, which improve the EE, while in case of $\rho = 0.9$ means that 0.1 of the transmitted power from the relay will reach to the destination, so the EE decreases. The steady-state convergence occurred after the initial ten iterations.

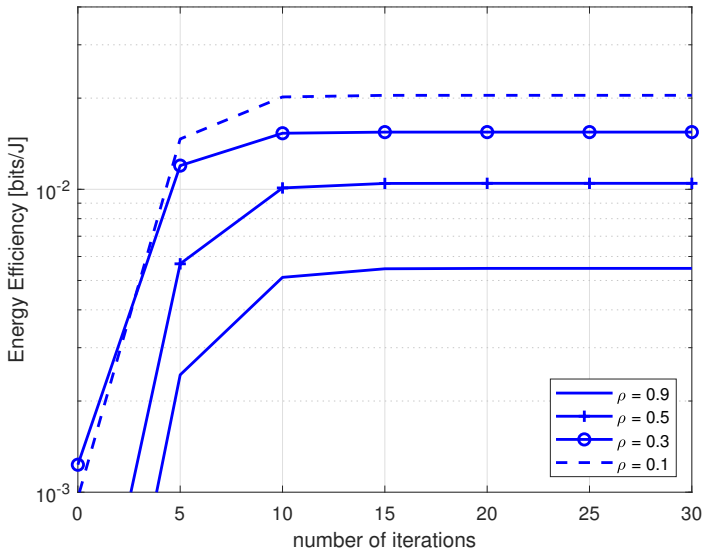

Figure 8. EE at 20 dB versus different power splitting ratio.

Figure 9 shows the EE of conventional and WEH relaying systems for different N relays. It is evident that EE performs better by increasing the relays. For example, at 10 dB SNR for WEH relaying, the EE is approximately 0.07 bits/J and 0.1 bits/J for $N = 2$ and $N = 5$, respectively. On the other hand, EE for WEH relaying outperformed conventional relaying; for example at 10 dB SNR and $N = 2$, the EE is approximately 0.01 bits/J and 0.07 bits/J for conventional and WEH relaying, respectively. Notably, EE for conventional relaying starts at approximately 10^{-3} bits/J at low SNR, whereas EE for WEH relaying is approximately 10^{-2} bits/J. According to [49], EE performs better in WEH relaying than in conventional relaying. For the low-SNR region, the EE of EH relaying increases faster than conventional relaying. This result leads to the conclusion that WEH relaying is the optimum solution for energy-constrained systems.

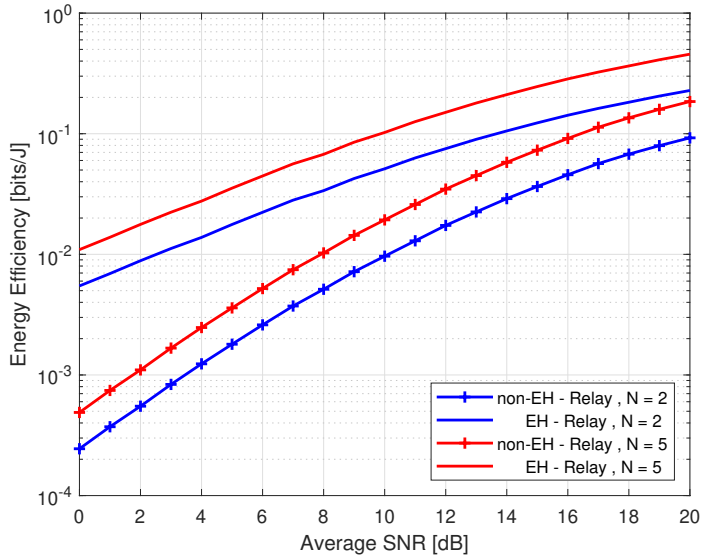

Figure 9. EE of conventional relaying and WEH relaying versus SNR for different N.

The relationship shown in Figure 10 illustrates the SE-EE trade-off metric. It is clear that there is an initial simultaneous increase of SE and EE, indicating the absence of a trade-off in this interval. The SE and EE trade-off starts at the point of inflection, followed by a decrement in EE along with SE. The square markers indicate that only EE is considered in the design of the wireless networks, while diamond markers indicate that only SE is considered. The region between square markers and diamond markers illustrates the trade-off between SE and EE. As shown, the maximum SE for WEH and non-WEH occurred at 1.4 bits/s/Hz and 2 bits/s/Hz, respectively, while the maximum EE for WEH and non-WEH occurred at 0.6 bits/s/Hz and 1.1 bits/s/Hz, respectively. According to [50], the SE-EE trade-off metric leads to a reduction in the energy consumed and transceiver architecture, thereby improving the complexity involved in the process and reducing the cost of operation. The SE-EE trade-off metric in [50] is shown for the non-WEH relay, while in this work, the WEH relay is shown and compared with the non-WEH relay. As expected, EE is better for the WEH relay than the non-WEH relay.

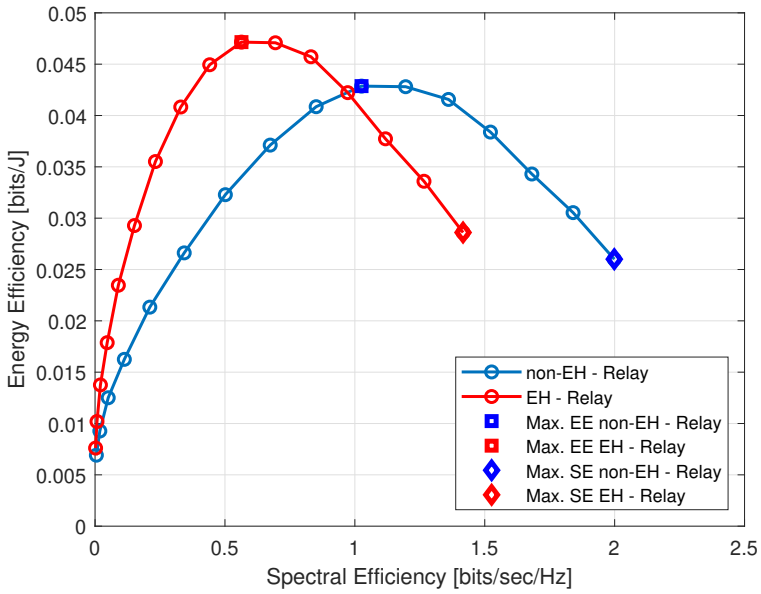

Figure 10. The SE-EE relationship for non-EH and EH relaying, $N = 5$.

6. Conclusions

In this paper, spectral and energy efficiency in AF-WEH relaying are investigated. We have formulated end-to-end SNR for WEH relaying and compared it with conventional CR over the BRS scheme to compute the SE over link adaptation networks for the optimal power-splitting ratio. The simulation results have shown that the WEH relaying performs better than conventional relaying especially at low SNR, which leads to optimum solutions for energy-constrained systems. Finally, the SE-EE trade-off metric is shown for both non-WEH and WEH relaying systems.

From a green communication perspective, our work combines different research trends like EH, EC, SE and EE over the SWIPT system. The significant finding from this paper indicates the potential of WEH technique, which can be applied in energy-constrained wireless CR systems and is expected to solve the problem of the conventional battery-operated relay in future 5G wireless networks, such as machine type communications and device-to-device communication. Wireless EH relaying can be employed in a scenario in which the machine type communications requests for device-to-device relays to forward the data to the machine type communications devices due to limited energy. In such a scenario, our proposed technique can significantly improve the EE compared to battery operated relaying. Multiple antenna system at the relay is expected to offer better performance than the single antenna relay employed in this work. As such, it can be the potential extension to our current works.

Moreover, the effects of a different fading channel environment, such as Rician fading on the proposed system can also be considered for future works.

Author Contributions: Formal analysis, A.A.; Methodology, A.A.; Software, A.A.; Supervision, R.N.; Writing—original draft, A.A.; Writing—review and editing, R.N. and M.I.

Funding: This research received no external funding.

Acknowledgments: The authors would like to thank Centre of Research and Instrumentation (CRIM) and Faculty of Engineering and Built Environment, Universiti Kebangsaan Malaysia (UKM) for their generosity in financial assistance.

Conflicts of Interest: The authors declare no conflict of interest.

Abbreviations

The following abbreviations are used in this manuscript:

5G	Fifth Generation
RF	Radio-Frequency
AWGN	Additive White Gaussian Noise
3GPP	Third Generation Partnership Project
EH	Energy Harvesting
BRS	Best Relay Selection
CR	Cooperative Relaying
EC	Energy Consumption
EE	Energy Efficiency
SE	Spectral Efficiency
SNR	Signal to Noise Ratio
AF	Amplify-and-Forward
DF	Decode-and-Forward
SWIPT	Simultaneous Wireless Information and Power Transfer
GSM	Global System for Mobile
LTE	Long Term Evolution
LTE-A	Long Term Evolution-Advanced
OP	Outage Probability
PS	Power Splitting
TS	Time Switching
MOP	Multi-Objective Optimisation problem
SOP	Single-Objective Optimisation problem
IOT	Internet of things
MSR	Multicast Secrecy Rate
WPT	Wireless Power Transfer
WPCNs	Wireless Powered Communication Networks
ICT	Information and Communication Technolog
PFUF	Proportional Fairness Utility Function
SC	Selection Combining
MRC	Maximal Ratio Combining
MAC	Multiple Access Channel
PAC	Parallel Access Channel
CMAC	Cooperative MAC
CPAC	Cooperative PAC
DFC	Decision Fusion Center
DaF	Decode-and-Fuse
DtF	Decode-then-Fuse
CJ	Cooperative Jamming
ARP	All Relay Participate
GA	Genetic Algorithm
CSI	Channel State Information

Appendix A. Derivation of Outage Probability

$$P_2 = Pr\left(\gamma_{brs} < \Gamma^{th}\right) = Pr\left(\frac{aX^2Z}{\overline{\rho}bXZ + bXZ + cX + \overline{\rho} + 1} < \Gamma^{th}\right), \tag{A1}$$

$$\begin{aligned}
&\frac{aX^2Z}{\overline{\rho}bXZ + bXZ + cX + \overline{\rho} + 1} < \Gamma^{th} \\
&\longrightarrow aX^2Z < (Z(\overline{\rho}bX + bX) + cX + \overline{\rho} + 1)\Gamma^{th} \\
&\longrightarrow \left[aX^2 - (b\Gamma^{th}\overline{\rho} - b\Gamma^{th})X\right] Z < (cX + \overline{\rho} + 1)\Gamma^{th}
\end{aligned}$$

$$P_2 = \int_0^{\infty} Pr\left[aX^2 - (b\Gamma^{th}\overline{\rho} - b\Gamma^{th})X\right] Z < (cX + \overline{\rho} + 1)\Gamma^{th} f(X)dX \tag{A2}$$

(a) The case when $aX^2 - (b\Gamma^{th}\overline{\rho} - b\Gamma^{th})X < 0$

$$\begin{aligned}
&aX < (b\Gamma^{th}\overline{\rho} - b\Gamma^{th}) \\
&X < \mu \\
&\mu = \frac{(b\Gamma^{th}\overline{\rho} - b\Gamma^{th})}{a} = \frac{\Gamma^{th}(2-\rho)}{\overline{\gamma}(1-\rho)}
\end{aligned}$$

In this case, the inequality $\left[aX^2 - (b\Gamma^{th}\overline{\rho} - b\Gamma^{th})X\right] Z < (cX + \overline{\rho} + 1)\Gamma^{th}$ holds for any X and Z therefore

$$Pr\left[aX^2 - (b\Gamma^{th}\overline{\rho} - b\Gamma^{th})X\right] Z < (cX + \overline{\rho} + 1)\Gamma^{th} = 1. \tag{A3}$$

(b) The case when $aX^2 - (b\Gamma^{th}\overline{\rho} - b\Gamma^{th})X > 0$

$$\begin{aligned}
&aX > (b\Gamma^{th}\overline{\rho} - b\Gamma^{th}) \\
&X > \mu
\end{aligned}$$

Then

$$\begin{aligned}
&Pr\left[aX^2 - (b\Gamma^{th}\overline{\rho} - b\Gamma^{th})X\right] Z < (cX + \overline{\rho} + 1)\Gamma^{th} \\
&= Pr\left[Z < \frac{(cX+\overline{\rho}+1)\Gamma^{th}}{\left[aX^2 - (b\Gamma^{th}\overline{\rho} - b\Gamma^{th})X\right]}\right] = Pr\left[Z < \Theta\right]
\end{aligned} \tag{A4}$$

where

$$\Theta = \frac{(cX + \overline{\rho} + 1)\Gamma^{th}}{\left[aX^2 - (b\Gamma^{th}\overline{\rho} - b\Gamma^{th})X\right]} \approx \frac{\xi}{X - \mu} \tag{A5}$$

$$\xi = \frac{(c + \overline{\rho} + 1)\Gamma^{th}}{a}, \tag{A6}$$

$$P_2 = \int_0^{\mu} f\left(X\right) dX + \int_{\mu}^{\infty} Pr\left(Z < \Theta\right) f\left(X\right) dX, \tag{A7}$$

$$\begin{aligned} P_2 &= \int_0^{\mu} f(X)\,dX + \int_{\mu}^{\infty}\left(1 - e^{-\Theta}\sum_{k=0}^{N-1}\frac{\Theta^k}{k!}\right) f(X)\,dX = \\ &= \int_0^{\mu} f(X)\,dX - \int_{\mu}^{\infty} e^{-\Theta}\sum_{k=0}^{N-1}\frac{\Theta^k}{k!} f(X)\,dX = \\ &= 1 - \int_{\mu}^{\infty} e^{-X}e^{-\Theta}\sum_{k=0}^{N-1}\frac{\Theta^k}{k!}dX = 1 - Q. \\ & u = X - \mu, \quad du = dX \end{aligned} \tag{A8}$$

$$\begin{aligned} Q &= \int_{\mu}^{\infty} e^{-X}e^{-\Theta}\sum_{k=0}^{N-1}\frac{\Theta^k}{k!}dX = \sum_{k=0}^{N-1}\frac{1}{k!}\int_{\mu}^{\infty} e^{-X}e^{-\Theta}\Theta^k dX = \\ &= \sum_{k=0}^{N-1}\frac{1}{k!}\int_{\mu}^{\infty} e^{-X}e^{-\frac{\xi}{X-\mu}}\frac{\xi^k}{(X-\mu)^k}dX = \\ &= \sum_{k=0}^{N-1}\frac{1}{k!}\int_{0}^{\infty} e^{-(u+\mu)}e^{-\frac{\xi}{u}}\frac{\xi^k}{u^k}du = \\ &= \sum_{k=0}^{N-1}\frac{\xi^k}{k!}e^{-\mu}\int_{0}^{\infty} u^{-k}e^{-\frac{\xi}{u}-u}du \end{aligned} \tag{A9}$$

from [51]

$$\int_0^{\infty} u^{-k}e^{-\frac{\xi}{u}-u}du = 2\xi^{\frac{1-k}{2}}K_{k-1}\left(2\sqrt{\xi}\right) \tag{A10}$$

$$Q = 2e^{-\mu}\sum_{k=0}^{N-1}\frac{\xi^{\frac{1+k}{2}}}{k!}K_{k-1}\left(2\sqrt{\xi}\right) \tag{A11}$$

$$P_2 = 1 - 2e^{-\mu}\sum_{k=0}^{N-1}\frac{\xi^{\frac{1+k}{2}}}{k!}K_{k-1}\left(2\sqrt{\xi}\right) \tag{A12}$$

Appendix B. Derivation of e2e SNR

$$\gamma_T = \frac{E_s|h_{sd}|^2}{d_3^n\sigma_{sd}^2} + \frac{E_iE_s\bar{\rho}|h_{si}|^2|h_{id}|^2d_1^{-n}d_2^{-n}}{\frac{E_i}{d_2^n}\bar{\rho}|h_{id}|^2\sigma_{si}^2 + \frac{E_i}{d_2^n}|h_{id}|^2\dot{\sigma}_{si}^2 + \sigma_{id}^2\bar{\rho}|h_{si}|^2\frac{E_s}{d_1^n} + \sigma_{id}^2\bar{\rho}\sigma_{si}^2 + \sigma_{id}^2\sigma_{si}^2} \tag{A13}$$

$$\gamma_T = E_s\nu_o + \frac{E_iE_s\bar{\rho}\zeta_i\nu_i}{E_i\bar{\rho}\zeta_i + E_i\zeta_i + E_s\bar{\rho}\nu_i + \bar{\rho} + 1} \tag{A14}$$

Then for N-relays (A14) can be written as

$$\gamma_T = E_s\nu_o + \sum_{i=1}^{N}\frac{E_iE_s\bar{\rho}\zeta_i\nu_i}{E_i\bar{\rho}\zeta_i + E_i\zeta_i + E_s\bar{\rho}\nu_i + \bar{\rho} + 1} \tag{A15}$$

After some mathematical manipulation

$$\gamma_T = E_s\nu_o + \sum_{i=1}^{N}E_s\nu_i - \sum_{i=1}^{N}E_s\nu_i + \sum_{i=1}^{N}\frac{E_iE_s\bar{\rho}\zeta_i\nu_i}{E_i\bar{\rho}\zeta_i + E_i\zeta_i + E_s\bar{\rho}\nu_i + \bar{\rho} + 1} \tag{A16}$$

$$\gamma_T = E_s\left(\nu_o + \sum_{i=1}^{N}\nu_i\right) - \sum_{i=1}^{N}\frac{E_s^2\nu_i\bar{\rho} + E_s\nu_iE_i\zeta_i + E_s\nu_i + E_s\nu_i\bar{\rho}}{E_i\bar{\rho}\zeta_i + E_i\zeta_i + E_s\bar{\rho}\nu_i + 1} \tag{A17}$$

For BRS scheme, (A17) can be written as (23).

References

1. Boyer, J.; Falconer, D.D.; Yanikomeroglu, H. Multihop diversity in wireless relaying channels. *IEEE Trans. Commun.* **2004**, *52*, 1820–1830. [CrossRef]
2. Halima, N.; Boujemaa, H. Exact and Approximate Symbol Error Probability of cooperative systems with best relay selection and all participating relaying using Amplify and Forward or Decode and Forward Relaying over Nakagami-m fading channels. *KSII Trans. Internet Inf. Syst.* **2018**, *12*, 81–108. [CrossRef]
3. Andrawes, A.; Nordin, R. Survey on performance of Adaptive Modulation scheme with cooperative Diversity in wireless systems. In Proceedings of the 2015 1st International Conference on Telematics and Future Generation Networks (TAFGEN), Kuala Lumpur, Malaysia 26–28 May 2015; pp. 65–70. [CrossRef]
4. Georgy, L.; Sergey, L. Amplify-and-forward versus decode-and-forward relaying: Which is better? In Proceedings of the 22th International Zurich Seminar on Communications (IZS), Zurich, Switzerland, 29 February–2 March 2012.
5. Touati, S.; Boujemaa, H.; Abed, N. Static hybrid multihop relaying and two hops hybrid relaying using DSTC. *Ann. Telecommun.* **2014**, *70*, 171–180. [CrossRef]
6. Tseng, S.; Liao, C. Distributed orthogonal and quasi-orthogonal space-time block code with embedded AAF/DAF matrix elements in wireless relay networks with four relays. *Wirel. Pers. Commun.* **2013**, *75*, 1178–1198. [CrossRef]
7. Zhang, R.; Ho, C.K. MIMO broadcasting for simultaneous wireless information and power transfer. *IEEE Trans. Wirel. Commun.* **2013**, *12*, 1989–2001. [CrossRef]
8. Zhou, X.; Zhang, R.; Ho, C.K. Wireless information and power transfer: Architecture design and rate-energy tradeoff. *IEEE Trans. Commun.* **2013**, *61*, 4754–4767. [CrossRef]
9. Li, C.; Song, S.H.; Zhang, J.; Letaief, K.B. Maximizing energy efficiency in wireless networks with a minimum average throughput requirement. In Proceedings of the 2012 IEEE Wireless Communications and Networking Conference (WCNC), Shanghai, China, 1–4 April 2012; pp. 1130–1134. [CrossRef]
10. Alsharif, M.H.; Nordin, R.; Ismail, M. Survey of green radio communications networks: Techniques and recent advances. *J. Comput. Netw. Commun.* **2013**, *2013*, 1–13. [CrossRef]
11. Huang, J.; Xing, C.; Wang, C. Simultaneous wireless information and power transfer: Technologies, applications, and research challenges. *IEEE Commun. Mag.* **2017**, *55*. [CrossRef]
12. Luo, S.; Zhang, R.; Lim, T.J. Optimal save-then-transmit protocol for energy harvesting wireless transmitters. *IEEE Trans. Wirel. Commun.* **2013**, *12*, 1196–1207. [CrossRef]
13. Miao, G.; Song, G. *Energy and Spectrum Efficient Wireless Network Design*, 1st ed.; Cambridge University Press: Cambridge, UK, 2014; doi:10.1017/CBO9781139626774.
14. Liu, L.; Zhang, R.; Chua, K.C. Wireless information and power transfer: A dynamic power splitting approach. *IEEE Trans. Commun.* **2013**, *61*, 3990–4001. [CrossRef]
15. Pervaiz, H.B.; Musavian, L.; Ni, Q.; Ding, Z. Energy and spectrum efficient transmission techniques under QoS constraints toward green heterogeneous networks. *IEEE Access* **2015**, *17*, 1655–1671. [CrossRef]
16. Fan, R.; Atapattu, S.; Chen, W.; Zhang, Y.; Evans, J. Throughput maximization for multi-hop decode-and-forward relay network with wireless energy harvesting. *IEEE Access* **2018**, *6*, 24582–24595. [CrossRef]
17. Gao, H.; Ejaz, W.; Jo, M. Cooperative wireless energy harvesting and spectrum sharing in 5G networks. *IEEE Access* **2016**, *4*, 3647–3658. [CrossRef]
18. Ahmed, I.; Ikhlef, A.; Schober, R.; Mallik, R.K. Joint power allocation and relay selection in energy harvesting AF relay systems. *IEEE Wirel. Commun. Lett.* **2013**, *2*, 239–242. [CrossRef]
19. Deng, Z.; Gao, Y.; Cai, C.; Li, W. Optimal transceiver design for SWIPT system with full-duplex receiver and energy-harvesting eavesdropper. *Phys. Commun.* **2018**, *26*, 1–8. [CrossRef]
20. Lee, J.H.; Sohn, I.; Kim, Y.H. Simultaneous wireless power transfer and secure multicasting in cooperative decode-and-forward relay networks. *Sensors* **2017**, *17*, 1128. [CrossRef] [PubMed]
21. Zhang, J.; Zhou, Q.; Ng, D.W.; Jo, M. Optimal energy efficiency fairness of nodes in wireless powered communication networks. *Sensors* **2017**, *17*, 2125. [CrossRef] [PubMed]
22. Rabie, K.; Salem, A.; Alsusa, E.; Alouini, M. Energy-harvesting in cooperative AF relaying networks over log-normal fading channels. In Proceedings of the 2016 IEEE International Conference on Communications (ICC), Kuala Lumpur, Malaysia, 22–27 May 2016; doi:10.1109/icc.2016.7511559. [CrossRef]

23. Zhang, Z.; Li, Y.; Huang, K.; Liang, C. Energy efficiency analysis of energy harvesting relay-aided cooperative networks. In Proceedings of the 2015 13th International Symposium on Modeling and Optimization in Mobile, Ad Hoc, and Wireless Networks (WiOpt), Mumbai, India, 25–29 May 2015; doi:10.1109/WIOPT.2015.7151025. [CrossRef]
24. Zhang, Q.; Jia, J.; Zhang, J. Cooperative relay to improve diversity in cognitive radio networks. *IEEE Commun. Mag.* **2009**, *47*, 111–117. [CrossRef]
25. Suraweera, H.; Smith, P.; Armstrong, J. Outage probability of cooperative relay networks in Nakagami-m fading channels. *IEEE Commun. Lett.* **2006**, *10*, 834–836. [CrossRef]
26. Adinoyi, A.; Yanikomeroglu, H. Cooperative relaying in multi-antenna fixed relay networks. *IEEE Trans. Wirel. Commun.* **2007**, *6*, 533–544. [CrossRef]
27. Bhatnagar, M. On the capacity of decode-and-forward relaying over rician fading channels. *IEEE Commun. Lett.* **2013**, *17*, 1100–1103. 2013.050313.12281. [CrossRef]
28. Salvo, P.; Ciuonzo, D.; Romano, G. Orthogonality and cooperation in collaborative spectrum sensing through MIMO decision fusion. *IEEE Trans. Wirel. Commun.* **2013**, *12*, 5826–5836. 2013.092013.130279. [CrossRef]
29. Ciuonzo, D.; Romano, G.; Rossi, P. Channel-aware decision fusion in distributed MIMO wireless sensor networks: Decode-and-Fuse vs. Decode-then-Fuse. *IEEE Trans. Wirel. Commun.* **2012**, *11*, 2976–2985. [CrossRef]
30. Ciuonzo, D.; Rossi, P.; Dey, S. Massive MIMO channel-aware decision fusion. *IEEE Trans. Signal Process.* **2015**, *63*, 604–619. [CrossRef]
31. Li, J.; Petropulu, A.; Weber, S. On cooperative relaying schemes for wireless physical layer security. *IEEE Trans. Signal Process.* **2011**, *59*, 4985–4997. [CrossRef]
32. Andrawes, A.; Nordin, R.; Ismail, M. Energy harvesting with cooperative networks and adaptive transmission. In Proceedings of the 2017 IEEE Jordan Conference on Applied Electrical Engineering and Computing Technologies (AEECT), Aqaba, Jordan, 11–13 October 2017; doi:10.1109/AEECT.2017.8257749.
33. Jiang, D.; Zhang, P.; Lv, Z.; Song, H. Energy-efficient multi-constraint routing algorithm with load balancing for smart city applications. *IEEE Internet Things J.* **2016**, *3*, 1437–1447.:10.1109/JIOT.2016.2613111. [CrossRef]
34. Lubritto, C.; Petraglia, A.; Vetromile, C.; Curcuruto, S.; Logorelli, M.; Marsico, G.; D'Onofrio, A. Energy and environmental aspects of mobile communication systems. *Energy* **2011**, *36*, 1109–1114. [CrossRef]
35. Kwon, H.; Birdsall, T. Channel capacity in bits per joule. *IEEE J. Ocean. Eng.* **1986**, *11*, 97–99. [CrossRef]
36. Chen, Y.; Zhang, S.; Xu, S.; Li, G.Y. Fundamental tradeoffs on green wireless networks. *IEEE Commun. Mag.* **2011**, *49*. [CrossRef]
37. Chih-Lin, I.; Rowell, C.; Han, S.; Xu, Z.; Li, G.; Pan, Z. Toward green and soft: A 5G perspective. *IEEE Commun. Mag.* **2014**, *52*, 66–73. [CrossRef]
38. Pan, C.; Xu, W.; Wang, J.; Ren, H.; Zhang, W.; Huang, N.; Chen, M. Totally distributed energy-efficient transmission in MIMO interference channels. *IEEE Trans. Wirel. Commun.* **2015**, *14*, 6325–6338. doi:10.1109/TWC.2015.2452908. [CrossRef]
39. Miao, G.; Himayat, N.; Li, Y.; Swami, A. Cross-layer optimization for energy-efficient wireless communications: A survey. *Wirel. Commun. Mob. Comput.* **2009**, *9*, 529–542.:4. [CrossRef]
40. Andrawes, A.; Nordin, R.; Ismail, M. Wireless Energy Harvesting with Amplify-andForward Relaying and Link Adaptation under Imperfect Feedback Channel. *J. Telecommun. Electron. Comput. Eng.* **2018**, *10*, 83–90.
41. Andrawes, A.; Nordin, R.; Ismail, M. Energy harvesting with link adaptation under different wireless relaying schemes. *J. Commun.* **2018**, *13*, 1–6. [CrossRef]
42. Alsharif, M.H.; Nordin, R.; Ismail, M. Intelligent cooperation management of multi-radio access technology towards the green cellular networks for the twenty-twenty information society. *Telecommun. Syst.* **2017**, *65*, 497–510. [CrossRef]
43. Liu, Y. Wireless information and power transfer for multi-relay assisted cooperative communication. *IEEE Commun. Lett.* **2015**, *20*, 784–787. [CrossRef]
44. Sesia, S.; Toufik, I.; Baker, M. *LTE—UMTS Long Term Evolution from Theory to Practice*, 2nd ed.; John Wiley and Sons: New York, NY, USA, 2011; doi:10.1002/9780470742891.
45. Andrawes, A. Performance of adaptive modulation with generalized selection combining in different practical scenarios. In Proceedings of the Seventh International Conference on Computer Engineering and Systems (ICCES), Cairo, Egypt, 27–29 November 2012; pp. 233–337. [CrossRef]
46. Simon, M.K.; Alouini, M.-S. *Digital Communication over Fading Channels*; John Wiley and Sons: New York, NY, USA, 2000; doi:10.1002/0471200697.

47. Avestimehr, A.S.; Tse, D.N.C. Outage capacity of the fading relay channel in the low-SNR regime. *IEEE Trans. Inform. Theory* **2007**, *53*, 1401–1415.:10.1109/TIT.2007.892773. [CrossRef]
48. di, x.; xiong, k.; zhang, y.; qiu, z. simultaneous wireless information and power transfer in two-hop OFDM decode-and-forward relay networks. *TIIS* **2016**, *10*, 152–167. [CrossRef]
49. Guo, S.; Zhou, X. Energy-efficient design in RF energy harvesting relay networks. In Proceedings of the 2015 IEEE Global Communications Conference (GLOBECOM), San Diego, CA, USA, 6–10 December 2015; doi:10.1109/GLOCOM.2015.7417800. [CrossRef]
50. Deng, L.; Rui, Y.; Cheng, P.; Zhang, J.; Zhang, Q.T.; Li, M. A unified energy efficiency and spectral efficiency tradeoff metric in wireless networks. *IEEE Commun. Lett.* **2013**, *17*, 55–58. [CrossRef]
51. Gradshteyn, I.S.; Ryzhik, I.M. *Table of Integrals, Series, and Products*, 7th ed.; Academic Press: San Diego, CA, USA, 2007; ISBN 9780471317791.